Electronic Supplementary Material (ESI) for Nanoscale.
This journal is © The Royal Society of Chemistry 2015

Nanoscale Supplementary Information

Electrical and Thermal Conduction in Ultra-thin Freestanding Atomic Layer Deposited W Nanobridges

S.1 Extracted Thermal Conductivity from Thermal Conductance Measurements

While there are various methods to measure thermal conductivity of structures and materials including the 3ω and frequency-dependent time-domain thermoreflectance, a simple DC based method has been used instead.[1,2] By measuring the thermal conductances (W K^{-1}) of a nanobridges with known physical dimensions, the thermal conductivity may be extracted by a model for joule heated nanobridges. By considering the 1-dimensional steady-state heat equation,

$$T''(x) = \frac{-Q(x)}{\kappa A}, \tag{S1}$$

where A is the total cross-sectional area of the bridge and the source Q(x) may be defined as,

$$Q(x) = j^2\rho, \tag{S2}$$

where j is current density (Amperes m^{-2}) and ρ is the temperature independent electrical resistivity. By applying the following definitions of j and ρ, Q(x) may be redefined:

$$j = \frac{I}{A}, \tag{S3}$$

$$\rho = R\frac{A}{l}, \tag{S4}$$

$$P = I^2R, \tag{S5}$$

$$Q(x) = \frac{P}{l}, \tag{S6}$$

where I is the current applied to the bridge, R is the resistance, l the length of the bridge, and P the total power applied. The solution to Equation S1 given the above joule heating conditions and boundary conditions T(0)=0 and T(l)=0 is given as,

$$T(x) = \frac{P}{2\kappa A}\left(x - \frac{x^2}{l}\right). \tag{S7}$$

To measure thermal conductance, the temperature of the bridge must be measured as power is applied by joule heating. The temperature may be calculated by using a known TCR value and by measuring the change in resistance of the bridge as the power applied. The average temperature of the bridge is given as,

$$\Delta T_{avg} = \frac{R_{avg} - R_o}{TCR \cdot R_o}, \tag{S8}$$

where R_{avg} is the measured resistance and R_o the initial resistance. By plotting power applied versus the average change in temperature of the beam, the thermal conductance (W K^{-1}) may be extracted by a linear fit (assuming a temperature independent thermal conductivity). To define the thermal conductance in terms of the thermal conductivity, the average of Equation S7 must be calculated since the temperature is calculated by measuring the average resistance of the bridge. The average change in temperature of the beam is given as,

$$\bar{T}(x) = \frac{Pl}{12\kappa A}, \tag{S10}$$

where thermal conductance is defined as,

$$G = \frac{P}{\bar{T}(x)} = 12\kappa\frac{A}{l}. \tag{S11}$$

A factor of 12 is introduced to the traditional definition of thermal conductance by the conditions of joule heating. Equation S11 may be utilized to fit thermal conduction versus nanobridge length demonstrated by Figure S1. Since the TCRs of the films investigated are extremely small,

(-0.015, -0.012 and -0.009 % K^{-1} for 11.55, 15.40 and 20.40 nm W films respectively) the temperature independent resistivity term may be utilized in the 1-D heat equation. Using a temperature dependent resistivity term in the derivation of average temperature presented above results in only a 1% difference in the extracted thermal conductivity value for the films measured here.

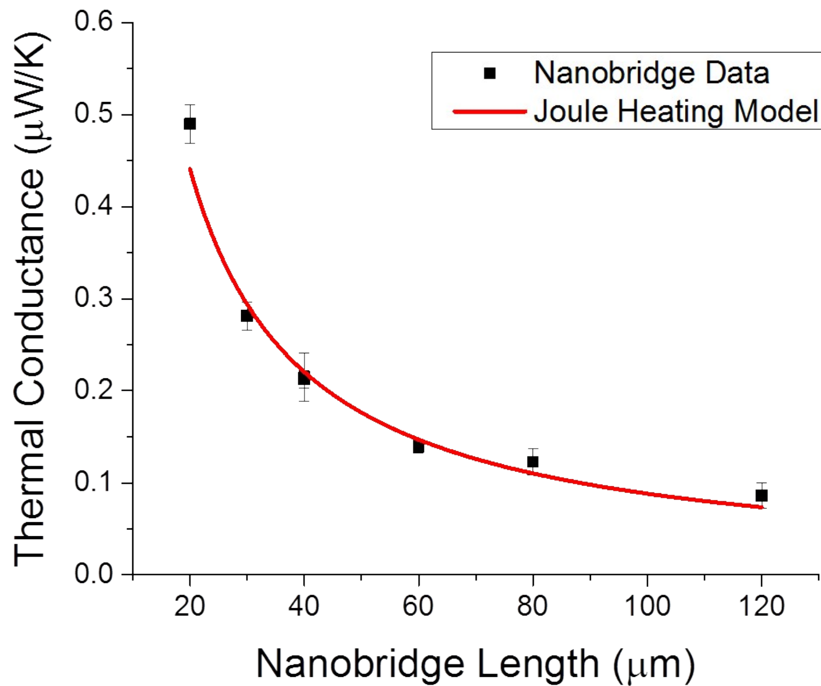

Figure S1. Relation of thermal conductance to length for a 9.8 nm Al_2O_3/20.40 W/9.8 Al_2O_3 cross-section nanobridge. Thermal conductivity is extracted by fitting the derived joule heating model (Equation S11) to the data.

S.2 Accuracy Test of Thermal Conductivity Extraction Method

To test the accuracy of the experimental method, nanobridge structures were fabricated out of a 100 nm thick aluminum film prepared by thermal evaporation. The film was prepared in a method similar to Volkov et al. in order to compare results of their measured thermal conductivity using joule heating and electron diffraction patterns.[3] The fabrication process was

similar to the one described in the manuscript, except that the contact pad and nanobridge structure were both made up of a single layer of 100 nm evaporated aluminum. The aluminum bridges were wet etched using "Transene A" Al etchant for ~ 4 minutes. Next, the TCRs of individual beams were tested in an unreleased state with a 100 μA test current to minimize joule heating. However, due to the low resistivity of aluminum, there was likely a negligible amount of joule heating even at higher bias currents. The measured TCR of the 100 nm Al sample was 0.3945 % K^{-1}. Thermal conductance measurements of released bridges were carried out as described in Section S.1. The wet etch resulted in varying widths of bridges and thus thermal conductivity was extracted through a plot of Thermal Conductance/Bridge Width vs. Bridge length where bridge widths were measured using an SEM. Figure S2 shows the Al bridge data and the joule heating model fit. The extracted value for the 100 nm Al film was 209.8 ± 4.7 W/mK. Volkov et al. measured 50, 74 and 110 nm films where the expected thermal conductivity for a 100 nm film based off their other 3 measurements was ~ 214 W/mK. Slight differences in thermal conductivity values are expected due to small variances in the film preparation method. However, the method presented in this manuscript was shown to extract a thermal conductivity value of 100 nm aluminum within 1.5% of work by Volkov et al..

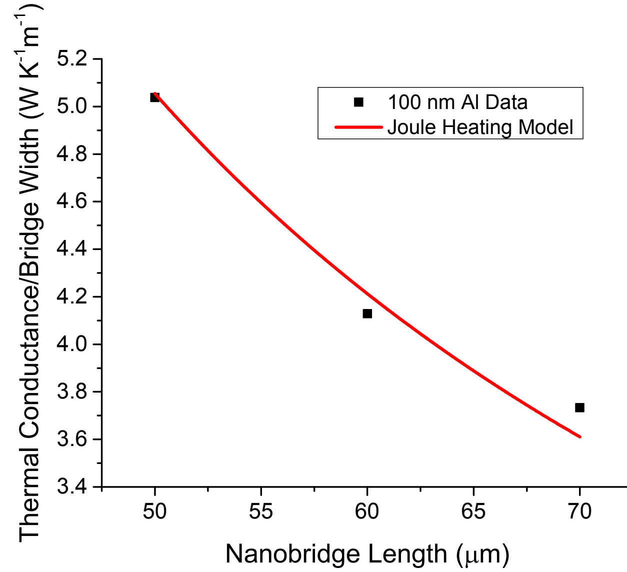

Figure S2. Relation of thermal conductance/bridge width to length for 100 nm Al film. Thermal conductivity is extracted by fitting the derived joule heating model (Equation S11) to the data.

S.3 Thermal Conductance Losses and Compensation Method

The previously described methods for measuring thermal conductances are done under vacuum at ~ 35 mTorr. Though thermal convection is negligible at this pressure, thermal losses such as conduction to the air and radiation must be considered.[4,5] Thermal conduction to air may be defined by the following relation,

$$G_{gas} = G_s + G_w = \frac{S}{\frac{1}{h_{s,hi}} + \frac{1}{h_{s,lo}}} + \frac{S}{\frac{1}{h_{w,hi}} + \frac{1}{h_{w,lo}}}, \tag{S12}$$

where G_s is the total conduction to the substrate from the bottom of the bridge, G_w is the total conduction to the substrate from the top of the bridge, S is the surface area of the nanobridge, $h_{s,hi}$ is the convection coefficient at ambient pressure between the bottom of the bridge and the substrate, $h_{s,lo}$ is the convection coefficient at low pressure between the bottom of the bridge, $h_{w,hi}$ is the convection coefficient at ambient pressure between the bridge and the window of the vacuum probe station, $h_{w,lo}$ is the convection coefficient at low pressure between the top of the

bridge and the window of the vacuum probe station. The heat convection coefficients may be defined as,

$$h = \frac{\kappa(P,d)}{d}, \qquad \text{(S13)}$$

where κ is the gas conductivity of air and is a function of pressure P, and distance d, to a theoretical parallel plate (substrate or viewing window). The thermal conductivity may be calculated by the following relation,

$$\kappa = \frac{\kappa_o}{1 + \frac{C}{PP}},^{6} \qquad \text{(S14)}$$

where C is a constant defined as 7.6 x 10^{-5} N m^{-1} K^{-1} and pressure parameter PP, is defined as,

$$PP = \frac{P \cdot d}{T},^{6} \qquad \text{(S15)}$$

where T is the absolute temperature. The conduction to air calculations were verified by measuring the thermal conductance of a beam at both 30 mTorr and 500 μTorr. The thermal conductance at 30 mTorr was 1.4% larger than the thermal conductance at 500 μTorr, only a 0.1 % difference from the calculations presented above.

Additionally, considering the large surface area to volume ratio for these ultra-thin nanobridges, radiation losses will become non-negligible as the bridges are heated. Radiation conduction may be defined as,

$$G_{rad} = 2 \cdot \sigma \cdot \varepsilon \cdot S \cdot T_{avg}^{3}, \qquad \text{(S16)}$$

where σ is the Stefan Boltzmann constant, and ε the emissivity, which is assumed to be 0.9 and background radiation is at ambient. However, even at the ~ 100K maximum temperature rise, the effects due to radiation is ~ 2 orders of magnitude smaller than the measured thermal conductances.

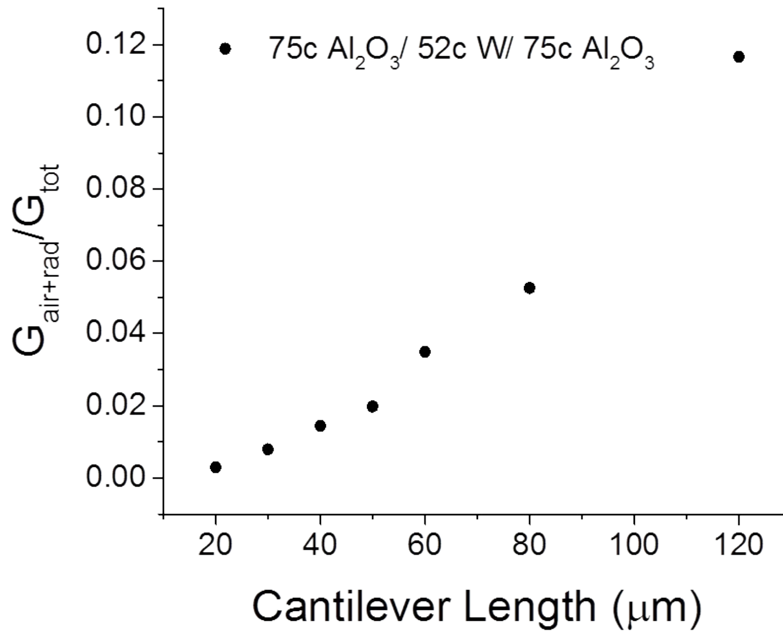

Figure S3. The percentage of conduction attributed to air and radiation from the total measured thermal conductance of individual nanobridges.

By combining the relevant conduction mechanisms of the nanobridge system under investigation, the total conduction may be defined as,

$$G_{tot} = G_{gas} + G_{rad} + G_{conv} + G_{beam}, \qquad \text{(S17)}$$

where G_{conv} is still negligible. An example of the percentage of bridge conduction attributed to conduction to air and radiation conduction for nanobridges with a 9.8 nm Al_2O_3/20.40 nm W/9.8 nm Al_2O_3 cross-section is shown in Figure S3.

For each sample, the total measured thermal conductance may be adjusted through the calculations described above. Figure S4 shows a plot of adjusted thermal conductance values and total thermal conductance values versus nanobridge length. Each data set was fit using the joule heating model presented in section S.1. For example, for a 9.8 nm Al_2O_3/20.40 nm W/9.8 nm Al_2O_3 cross-sectional nanobridge, the relative change in thermal conductivity was reduced by 1.8%.

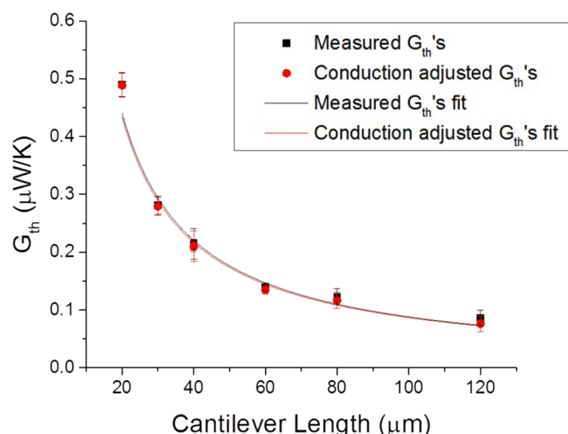

Figure S4. Adjusted thermal conductance values and total measured thermal conductance values with associated fits using the joule heating model from section S.1.

S.4 XRD Measurement and Modeling of W Grain Size

This section of supporting info discusses the methods used to measure and interpret the grain size of several thickness (ALD cycles) of W films. The ALD cycles correspond to the same thickness range as discussed in the paper. Grazing Incidence X-ray Diffraction (GIXRD) and the Scherrer equation were used to estimate crystal grain sizes in the W films from the amount of peak broadening in the X-ray diffraction peaks. GIXRD spectra indicate the presence of β-W in the ALD films, and it is likely that a mixture of both β-W and α-W exist. It is difficult, however, to accurately separate the four GIXRD peaks necessary for using the Scherrer equation, but a lower limit on grain size can be obtained by fitting the entire broad spectrum, from an Omega of 30 to 50, as one single peak (see Figure S5 and Figure S6).

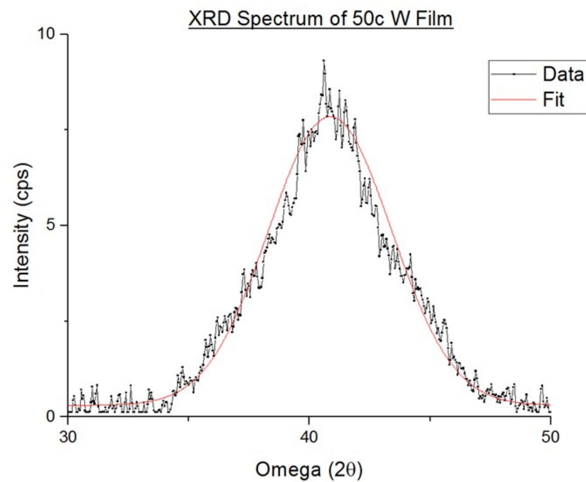

Figure S5. XRD data showing a single peak fit on a 20 nm W ALD film.

The Scherrer equation for crystal grain size, S, is given by

$$S = \frac{0.9\lambda}{B\cos(\theta)}, \qquad \text{(S18)}$$

where λ is the X-ray radiation used (here 1.541 Å), B is the full width at half max of the 2θ peak in radians, and θ is half of the omega angle at which the peak max occurs. If, instead, four peaks

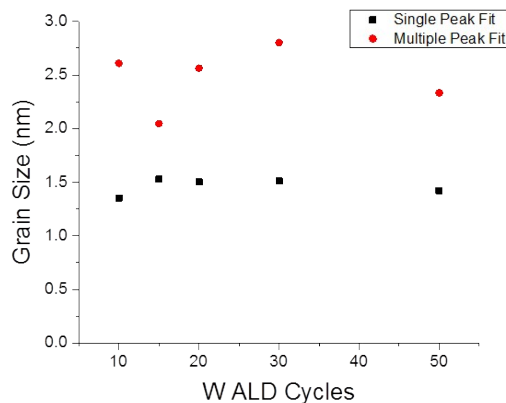

Figure S6. Grain size relation to W ALD cycles (thickness). Black data points are from a single peak fit of GIXRD data. Red data points are from an averaged multiple peak fit of GIXRD data for various phases of ALD W.

(three β-W peaks and one α-W peak) are used to fit the GIXRD spectrum from 30 to 50 Omega, a larger estimated grain size is obtained. Figure S7 shows a four-peak fit. Red data points in

Figure S6 are an average over all three β-W peaks using the four-peak fit. The average grain size between each method of analysis is ~ 2 nm, which was used in the electrical and thermal conduction modeling of W films. Results show no significant dependence on crystal grain sizes when changing the W thickness for the film thicknesses considered, regardless of fitting method.

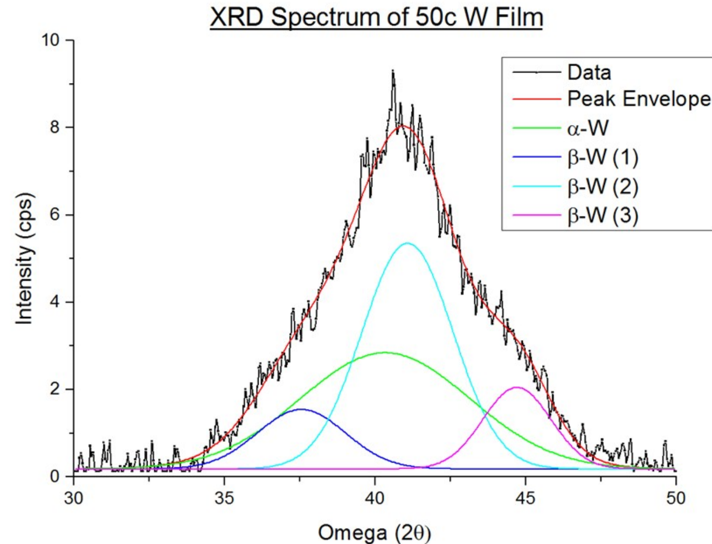

Figure S7. Example of a multiple peak fitting for the XRD spectrum of the 20 nm W film.

References:

[1] S. Yoneoka, J. Lee, M. Liger, G. Yama, T. Kodama, M. Gunji, J. Provine, R. T. Howe, K. E. Goodson and T. W. Kenny, *Nano Lett.*, 2012, **12**, 683–686.

[2] J. Liu, B. Yoon, E. Kuhlmann, M. Tian, J. Zhu, S. M. George, Y.-C. Lee and R. Yang, *Nano Lett.*, 2013, **13**, 5594–5599.

[3] Y. A. Volkov, L. S. Palatnik and A. T. Pugachev, *Zh Eksp Teor Fiz*, 1976, **70**, 2244–2250.

[4] A. S. I World Congress on Engineering and International Association of Engineers, Eds., *World Congress on Engineering: WCE 2010 : 30 June - 2 July, 2010, Imperial College London, London, U.K.*, Newswood Ltd. ; International Association of Engineers, Hong Kong, 2010.

[5] M. M. Sisto, S. García-Blanco, L. Le Noc, B. Tremblay, Y. Desroches, J.-S. Caron, F. Provencal and F. Picard, in *SPIE*, eds. R. C. Kullberg and R. Ramesham, 2010, vol. 7592, pp. 759204–759204–10.

[6] *Fluid Flow Databook*, Genium Publishing, 1982.